


RESEARCH ARTICLE | MARCH 18 2022

## Oil-water separation in a cylindrical cyclone with vortex finder

Jian Zhang (张健)  Yun-teng He (何云腾); Shuo Liu (刘硕); ... et. al



*Physics of Fluids* 34, 033314 (2022)

<https://doi.org/10.1063/5.0085029>



Export  
Citation

CrossMark

### Articles You May Be Interested In

Numerical study of the effect of vortex finder configuration in dense medium cyclones

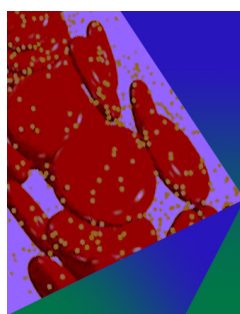
*AIP Conference Proceedings* (March 2010)

Oil–water two-phase flow-induced vibration of a cylindrical cyclone with vortex finder

*Physics of Fluids* (April 2023)

The investigation of the failed duplex material and remaining life prediction of vortex finder Cyclone in the circulating fluidized bed boiler

*AIP Conference Proceedings* (February 2023)



## Physics of Fluids

### Special Topic: Flow and Forensics

Submit Today!

# Oil-water separation in a cylindrical cyclone with vortex finder

Cite as: Phys. Fluids **34**, 033314 (2022); doi: [10.1063/5.0085029](https://doi.org/10.1063/5.0085029)

Submitted: 12 January 2022 · Accepted: 27 February 2022 ·

Published Online: 18 March 2022




View Online



Export Citation



CrossMark

Jian Zhang (张健),<sup>1,2,a)</sup>  Yun-teng He (何云腾),<sup>1</sup> Shuo Liu (刘硕),<sup>1,2</sup> and Jing-yu Xu (许晶禹)<sup>1,2,a)</sup>

## AFFILIATIONS

<sup>1</sup>Institute of Mechanics, Chinese Academy of Sciences, Beijing 100190, China

<sup>2</sup>School of Engineering Sciences, University of Chinese Academy of Sciences, Beijing 100049, China

<sup>a)</sup>Author to whom correspondence should be addressed: [zhangjian@imech.ac.cn](mailto:zhangjian@imech.ac.cn) and [xujingyu@imech.ac.cn](mailto:xujingyu@imech.ac.cn)

## ABSTRACT

Cylindrical cyclones are always used in the petroleum industry to separate the oil-water two-phase mixtures or treatment the waste water. Here, we use dimensional analysis and multiphase flow numerical simulation to analyze the separation process in a cylindrical cyclone with a vortex finder to better understand the theory and characteristics of separation. In the dimensional analysis, we consider all structural, flow, and operating parameters. A multiphase mixture model is used to simulate oil-water two-phase flow and separation in a cylindrical cyclone. There is a vortex in the core of the cylinder, and its structure is influenced by the diameter of the overflow pipe, the inlet velocity, and the flow split ratio. However, the influence of these three factors on the equivalent diameter of the vortex core can be ignored. Moreover, the inlet velocity has little influence on the equivalent length of the vortex core. Therefore, the structure of the vortex core can be calculated from the diameter and flow split ratio of the up-outlet of the cylindrical cyclone. Oil-water separation increases as the diameter of the oil droplet increases. The separation efficiency of the cylindrical cyclone with vortex can reach 80% if the inlet dispersion droplet diameter is larger than 1 mm. The oil volume fractions in the up- and down-outlets decrease as the overflow split ratio increases. The flow split ratio is the only operating parameter to consider to obtain the best separation results for a cylindrical cyclone with a fixed inlet oil-water mixture.

© 2022 Author(s). All article content, except where otherwise noted, is licensed under a Creative Commons Attribution (CC BY) license (<http://creativecommons.org/licenses/by/4.0/>). <https://doi.org/10.1063/5.0085029>

## I. INTRODUCTION

Water and crude oil coexist in the petroleum industry, and the water volume fraction increases as producing wells age. Some oil-water mixtures exist in the form of oil-in-water or water-in-oil emulsions.<sup>1</sup> The efficiency of oil-water separation technology greatly affects the economics of petroleum mining.<sup>2</sup> Current oil-water separation relies on the classic vessel-type separator, which is generally bulky, heavy, expensive, and inefficient. To improve the efficiency of petroleum exploitation, smaller, lighter, and more efficient separators are needed.

Centrifugal separation, which exploits the difference in density between oil and water, is one of the most efficient methods of separating oil and water.<sup>3</sup> The hydrocyclone is the classic centrifugal separation technology, and plenty of research has been done on it.<sup>4,5</sup> The cylindrical cyclone is one of the most significant developments in liquid-liquid two-phase centrifugal separation technology.<sup>6</sup> It functions much like the traditional hydrocyclone but is easier to control and appropriate for a wider range of fixed-size equipment because its underflow outlet is designed on the tangent of the cylinder.<sup>7</sup>

Researchers have used theoretical analysis, experimentation, and numerical simulation to better understand separation in cylindrical cyclones. Afanador<sup>8</sup> was the first to develop the concept of the liquid-liquid cylindrical cyclone. Experiments and numerical simulations of its flow behavior suggested that the cylindrical cyclone can efficiently achieve two-phase separation. Oropeza-Vazquez *et al.*<sup>9</sup> researched the hydrodynamics of oil-water two-phase flow in a cylindrical cyclone experimentally and theoretically. They showed that clean water can be obtained in the underflow but incomplete separation occurs in the cylindrical cyclone. For the fixed inlet flow, an optimal split ratio exists that depends on the inlet two-phase flow pattern. Also, they developed a new mechanism model to predict the efficiency of the separation of two-phase flow in a cylindrical cyclone. Mathiravedu *et al.*<sup>10</sup> studied the control of a liquid-liquid cylindrical cyclone in industrial applications. Their developed control method resulted in clear water in the underflow outlet and maintained the maximum underflow rate at the same time. Liu *et al.*<sup>11</sup> used numerical methods to study the flow field characteristics of a cylindrical cyclone. The Euler-Euler multiphase flow model and Reynolds stress turbulence model were used in their

numerical simulation. They found that the low-pressure zone in the core of the cylinder can create an upward flow to the overflow outlet. Moreover, a series of experiments have been done on oil-water two-phase separation in a cylindrical cyclone. The process for separating oil and water is given in the literature. In addition, the effect of the Reynolds number and flow split ratio on the separation efficiency was investigated by dimensional analysis, which can be used to predict the separation result. Gao *et al.*<sup>12</sup> studied the effect of a vortex on the flow behaviors of a cylindrical cyclone and presented a method of analyzing vortex structure using the Q criterion. The method shows that the hydraulic diameter of the vortex decreases from the upper region to the down-outlet along the axis of the cylindrical cyclone. It is useful for understanding oil-water two-phase flow behavior in a cylindrical cyclone.<sup>13</sup>

Here, we use dimensional analysis to analyze oil-water two-phase flow and separation in a cylindrical cyclone with vortex finder. To better understand the process and consequences of two-phase separation, we use numerical simulation to research factors that affect the vortex core of the cylindrical cyclone. Also, we use numerical simulation to study oil-water two-phase separation to verify the results of our theoretical analysis. It is important to understand the separation behavior of the cylindrical cyclone.

## II. THEORETICAL ANALYSIS

To determine the flow and separation mechanisms of the cylindrical cyclone with vortex finder, we first use dimensional analysis to analyze the relevant processes. The phase distribution is the direct performance to analyze the separation process.<sup>14,15</sup> Figure 1 shows a schematic diagram of a cylindrical cyclone with vortex finder. Fluid flows

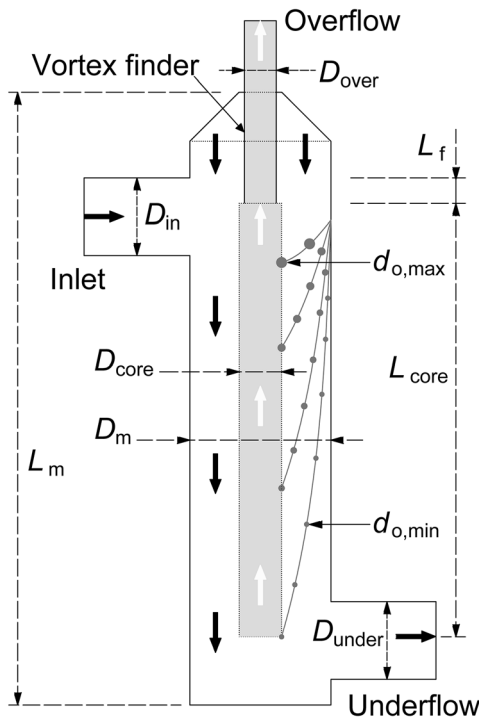


FIG. 1. Schematic diagram of a cylindrical cyclone with the vortex finder.

into the cyclone from the inlet with a tangential design, which creates a swirling field in the main cylinder. As a result of centrifugal force and the design of the two outlets, a core with upward axial velocity appears in the center of the cylinder, and at the same time, an annular flow with downward axial velocity appears near the wall of the cylinder.<sup>16</sup> Most of the fluid in the core flows out from the up-outlet, and the fluid in the outside flows out from the down-outlet. The diameter and length of the core are influenced by the structural and operating parameters. For oil-water two-phase flow and separation in a cylindrical cyclone, the oil phase must flow into the core if oil-water separation is to be realized under centrifugal force. The size of the oil droplet has a great influence on the separation efficiency.<sup>17</sup> There exists a minimum diameter of oil droplet that can be separated from the oil-water mixture by the cylindrical cyclone.<sup>18</sup> Therefore, the result of oil-water two-phase separation depends on the structure of the core and the diameters of the oil droplets.

The relevant parameters and their dimensions are as follows:

- Diameter of the inlet pipe,  $D_{in}$  (L)
- Contraction ratio of the tangential inlet,  $\varepsilon$  (–)
- Diameter of the main cylindrical pipe,  $D_m$  (L)
- Diameter of the overflow pipe,  $D_{over}$  (L)
- Diameter of the underflow pipe,  $D_{under}$  (L)
- Length of the main cylindrical pipe,  $L_m$  (L)
- Length of the vortex finder,  $L_f$  (L)
- Inlet velocity,  $v_{inlet}$  (L/T)
- Overflow split ratio,  $\lambda_{over}$  (–)
- Diameter of the smallest oil droplet,  $d_{o,min}$  (L)
- Diameter of the largest oil droplet,  $d_{o,max}$  (L)
- Difference in density between oil and water,  $\Delta\rho$  (M/L<sup>3</sup>)

The length and diameter of the vortex core in the center of the cylinder, where the axial velocity is up to the overflow, can be expressed as follows:

$$[L_{core}, D_{core}] = f(D_{in}, \varepsilon, D_m, D_{over}, D_{under}, L_m, L_f, v_{inlet}, \lambda_{over}). \quad (1)$$

Three parameters,  $D_m$ ,  $v_{inlet}$ , and  $\Delta\rho$ , are selected as a basic unit system. The relationship above can be translated to a dimensionless form:

$$\left[ \frac{L_{core}}{D_m}, \frac{D_{core}}{D_m} \right] = f \left( \frac{D_{in}}{D_m}, \varepsilon, \frac{D_{over}}{D_m}, \frac{D_{under}}{D_m}, \frac{L_m}{D_m}, \frac{L_f}{D_m}, \frac{v_{inlet}}{D_m}, \lambda_{over} \right). \quad (2)$$

Following previous research,<sup>19</sup> the diameter of the inlet pipe is always equal to that of the main cylinder, and the diameter of the underflow pipe has little influence on flow and separation. The contraction ratio of the tangential inlet and the inlet velocity can be composited to one factor that just influences the centrifugal force together. Moreover, Ghodrati *et al.*<sup>20</sup> showed that the effect of the vortex finder length on separation is much less significant than the effect of diameter:

$$\left[ \frac{L_{core}}{D_m}, \frac{D_{core}}{D_m} \right] = f \left( \frac{D_{over}}{D_m}, \frac{L_m}{D_m}, \frac{v_{inlet}}{\varepsilon}, \lambda_{over} \right). \quad (3)$$

Therefore, we can see that the structure of the vortex core in the cylindrical cyclone is influenced by the overflow pipe diameter, the length of the cylinder, the inlet velocity and the flow split ratio. The flow split ratio is the only operable parameter. It is important to design the structure of a cylindrical cyclone. The relation between the structure of

the vortex core and these influences can be determined by direct simulations. The effects of  $D_{\text{over}}$ ,  $v_{\text{inlet}}$ , and  $\lambda_{\text{over}}$  are studied in this work.

Mantilla *et al.*<sup>21</sup> showed that the movement of a dispersed oil droplet depends on the tangential and axial velocities, and the radial flow of the continuous phase is ignored. The relative axial velocity ( $v_{a,r}$ ) and the radial velocity ( $v_{r,r}$ ), respectively, between continuous phase water and oil droplets can be calculated as follows:

$$v_{a,r} = \left[ \frac{4(\rho_m - \rho_o)d_o}{3\rho_w C_D} \right]^{1/2} \times g \times \left[ g^2 + \left( \frac{v_{\text{inlet}}^2}{D_m/2} \right) \right]^{-1/4}, \quad (4)$$

$$v_{r,r} = \left[ \frac{4(\rho_m - \rho_o)d_o}{3\rho_w C_D} \right]^{1/2} \times \frac{v_{\text{inlet}}^2}{D_m/2} \times \left[ g^2 + \left( \frac{v_{\text{inlet}}^2}{D_m/2} \right) \right]^{-1/4}. \quad (5)$$

The drag coefficient ( $C_D$ ) is always 0.44 for turbulent flow as in the two-phase flow in a cylindrical cyclone.

In oil-water two-phase separation, the oil droplet should first flow into the vortex core in the center of the cylinder. Therefore, the flow time of the oil droplet from the cylinder wall to the vortex core ( $t_r$ ) must be less than the flow time of the oil droplet from the inlet to the end of the vortex core ( $t_a$ ):

$$t_r \leq t_a, \quad (6)$$

$$\frac{(D_m - D_{\text{core}})}{2v_{r,r}} \leq \frac{L_{\text{core}} + L_f - D_{\text{in}}}{v_a - v_{a,r}}. \quad (7)$$

The axial velocity of the continuous water phase ( $v_a$ ) can be calculated as follows:

$$v_a = \frac{4Q_{\text{under}}}{\pi(D_m^2 - D_{\text{core}}^2)} = \frac{v_{\text{inlet}} D_{\text{in}}^2 (1 - \lambda_{\text{over}})}{(D_m^2 - D_{\text{core}}^2)}. \quad (8)$$

The smallest diameter of the separated oil droplet ( $d_{o,\text{min}}$ ) can be obtained by Eqs. (4)–(8). The result of oil-water two-phase separation in a cylindrical cyclone with vortex finder can be predicted if the sizes of the oil droplets are known. The oil volume fractions in the overflow ( $\varphi_{o,\text{over}}$ ) and underflow ( $\varphi_{o,\text{under}}$ ), respectively, can be calculated as follows:

$$\varphi_{o,\text{over}} = \frac{\varphi_{o,\text{inlet}} V_{o,d_o \geq d_{o,\text{min}}}}{\lambda_{\text{over}}} + \varphi_{o,\text{inlet}} (1 - V_{o,d_o \geq d_{o,\text{min}}}), \quad (9)$$

$$\varphi_{o,\text{under}} = \varphi_{o,\text{inlet}} (1 - V_{o,d_o \geq d_{o,\text{min}}}). \quad (10)$$

Here,  $\varphi_{o,\text{inlet}}$  is the inlet oil volume fraction and  $V_{o,d_o \geq d_{o,\text{min}}}$  is the volume fraction of the oil droplet whose diameter is larger than that of the smallest separated oil droplet.

### III. NUMERICAL METHODS

#### A. Multiphase flow model

Two flow models, the Euler–Lagrange model and the Euler–Euler model, are used in multiphase flow simulation.<sup>22</sup> The Euler–Lagrange model is used to calculate two-phase flow, where one of the phases is dispersed and the volume fraction of the dispersed phase is less than 0.1.<sup>23</sup> The Euler–Euler model, which is useful for describing double continuous two-phase flow, includes Euler, mixture, volume of fluid (VOF), and other interface capture models.<sup>24,25</sup> In the present study, the oil-water two-phase flow does not have a stable continuous interface between oil and water, and the dispersed phase

exhibits coalescence and is broken. Therefore, the mixture model is most suitable for calculating oil-water two-phase flow and separation behaviors in the cylindrical cyclone.

In the mixture model, the two phases are regarded as a single mixture phase, and the governing equation of the mixture is solved. The interfacial phenomenon is ignored, and slip velocity is introduced to describe the two-phase flow.<sup>26</sup> The density  $\rho_m$  and viscosity  $\mu_m$  of the mixture can be calculated as follows:

$$\rho_m = \sum_{k=1}^n \alpha_k \rho_k, \quad (11)$$

$$\mu_m = \sum_{k=1}^n \alpha_k \mu_k. \quad (12)$$

The continuity equation of the mixture is

$$\frac{\partial}{\partial t} (\rho_m) + \nabla \cdot (\rho_m \mathbf{u}_m) = 0, \quad (13)$$

where the velocity of the mixture can be calculated from the average values of each phase:

$$\mathbf{u}_m = \frac{\sum_{k=1}^n \alpha_k \rho_k \mathbf{u}_k}{\rho_m}. \quad (14)$$

The momentum equation of the mixture is

$$\begin{aligned} \frac{\partial}{\partial t} (\rho_m \mathbf{u}_m) + \nabla \cdot (\rho_m \mathbf{u}_m \mathbf{u}_m) \\ = -\nabla P + \nabla \cdot [\mu_m (\nabla \mathbf{u}_m + \nabla \mathbf{u}_m^T)] \\ + \rho_m \mathbf{g} + \mathbf{F} + \nabla \cdot \left( \sum_{k=1}^n \alpha_k \rho_k \mathbf{u}_{dr,k} \mathbf{u}_{dr,k} \right), \end{aligned} \quad (15)$$

where  $\mathbf{F}$  is the body force and  $\mathbf{u}_{dr,k}$  is the drift velocity of phase  $k$ ,

$$\mathbf{u}_{dr,k} = \mathbf{u}_k - \mathbf{u}_m. \quad (16)$$

#### B. Geometric model and grid generation

Following previous study, we design a cylindrical cyclone with vortex finder. It is made up of a tangential inlet, main cylinder, down-outlet, and up-outlet with the vortex finder. All structural parameters are shown in Table I. The diameter of the main cylinder and inlet is 100 mm, and the diameter of the down-outlet is 80 mm. The lengths of the main cylinder and vortex finder are 1250 mm and 150 mm, respectively. Three diameters of up-outlet pipe, 10 mm, 25 mm, and 50 mm, are used to research the influence of diameter on the flow field.

TABLE I. Structural parameters of the cylindrical cyclone with vortex finder.

Parameter	Value	Parameter	Value
$D_{\text{in}}$	100 mm	$D_{\text{under}}$	80 mm
$D_{\text{m}}$	100 mm	$D_{\text{over}}$	10/25/50 mm
$L_{\text{m}}$	1250 mm	$L_f$	150 mm

We generate the grid using the ICEM software platform. The three-dimensional geometric model is separated into four parts—inlet, main cylinder, up-outlet, and down-outlet—to create a grid for the model. The generated grid is shown in Fig. 2, and the O-blocking method is used to create the structure cell. In order to test the influence of cell size on the accuracy of the numerical simulation, three different scales of grid are generated. The numerical result of the axial velocity in the cross section of the main cylinder for different cell sizes is displayed in Fig. 3. It shows that the numerical consequence of the medium grid scheme is almost the same as the fine scheme, but the coarse scheme has a little difference to others. Thus, the medium grid scheme is chosen to promise the computational accuracy and efficiency at the same time. About 2.94 million elements are created for the model in this study.

### C. Solution setting and boundary conditions

For the numerical simulation, the RNG  $k$ - $\epsilon$  turbulence model is chosen and the equations are solved using the SIMPLE algorithm based on the finite volume method.<sup>27,28</sup> Given the oil-water two-phase mixture, the primary phase in the flow is set as water, whereas the second phase is set as oil because the inlet oil volume fraction is always less than 0.4 in our study. The physical properties of oil and water (i.e., density, viscosity, and surface tension) are shown in Table II. The difference in density between oil and water is  $138 \text{ kg/m}^3$ .

As for boundary conditions, the velocity inlet boundary is set for the flow entrance where the oil and water phases have their own inlet velocities, phase volume fractions. Also, the droplet diameter of the dispersed phase oil is set in the inlet flow boundary, which is

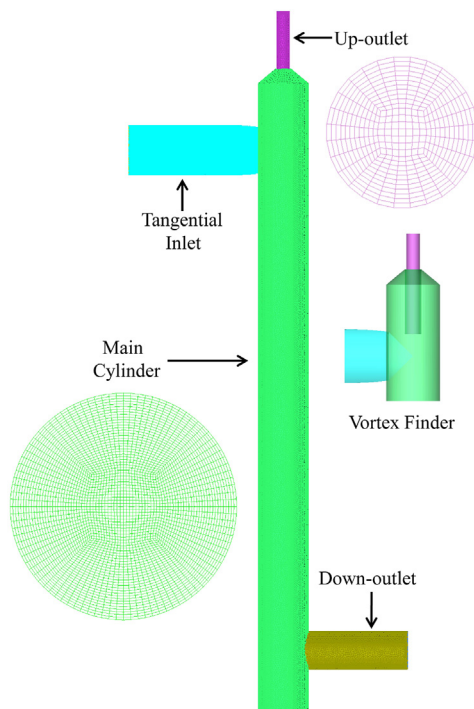


FIG. 2. Schematic diagram of the cylindrical cyclone with vortex finder.

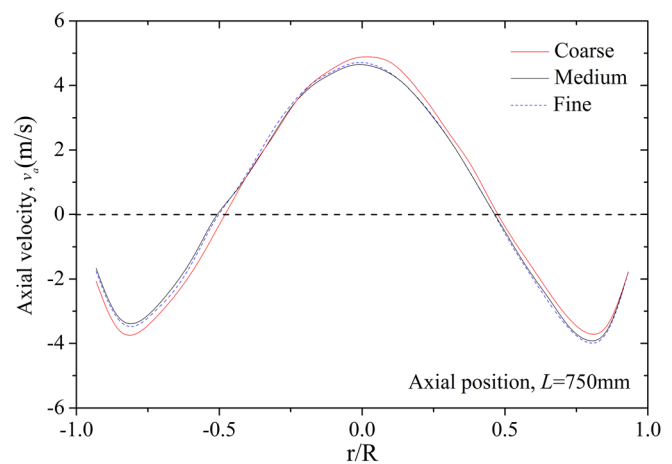


FIG. 3. The influence of the grid generation on the computational accuracy.

important to the oil-water separation. For the up- and down-outlets, the outflow boundary is selected to control the flow split ratio expediently. The other boundary conditions are the same as for a stationary wall with non-slip flow.<sup>29</sup> The steady solver is used in the numerical simulation because the oil-water inlet flow, and other boundary conditions are fixed.

## IV. FLOW FIELD ANALYSIS

### A. Flow field characteristics of the cylindrical cyclone

In line with the results of the mechanism analysis above, the flow field has a great influence on separation in the cylindrical cyclone with the vortex finder. We use numerical simulation to study in detail the flow field characteristics of the cylindrical cyclone. The diameter of the up-outlet is 25 mm. The inlet velocity is 2 m/s, and the overflow split ratio is 0.2. The results of numerical simulation of single-phase water flow in the cylindrical cyclone are used to accurately analyze the flow field characteristics.

The axial, tangential, and radial velocities in the cross section of the main cylinder are shown in Figs. 4–6, respectively. Figure 4 shows that the axial velocity is upward in the center of the cylinder and downward near the wall. This proves the accuracy of the consequence of the separation mechanism. However, the distribution of the axial velocity is not axisymmetric because of the asymmetrical inlet structure. The distributions of the tangential and radial velocities are approximately axisymmetric in the cross section. The direction of the radial velocity can transport the oil droplet to the core in the center of the main cylinder to achieve oil-water two-phase separation.

Figure 7 gives the static pressure and axial velocity in the axial line of the main cylinder. We can see that the static pressure in the

TABLE II. Physical properties of oil and water in this work ( $T = 30^\circ\text{C}$ ,  $P = 0.1 \text{ MPa}$ ).

	Density, $\text{kg/m}^3$	Viscosity, $\text{mPa}\cdot\text{s}$	Surface tension, $\text{N/m}$
Oil	860	85	0.042
Water	998	1	0.071



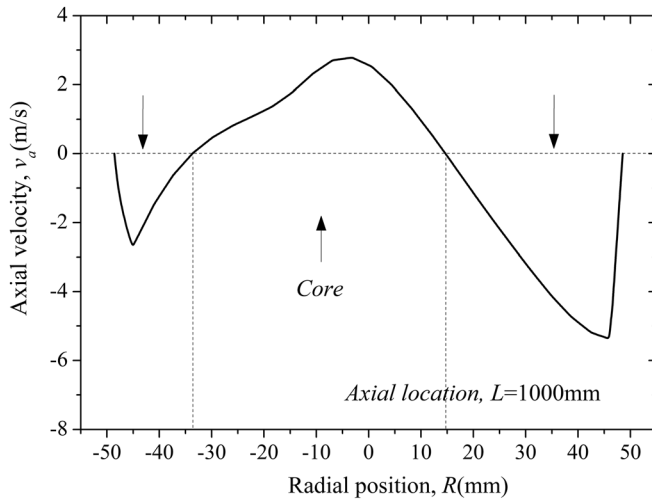


FIG. 4. The distribution of axial velocity in the cross section of the main cylinder.

axial line is negative, which can direct the radial velocity from the wall to the core. The static pressure decreases from the bottom up. In contrast, the axial velocity in the axial line increases from the down-outlet to the up-outlet. This explains the flow of the core in the center of the cylinder.

### B. The influence of the diameter of the overflow pipe

In this section, we consider the influence of the diameter of the overflow pipe on the structure of the vortex core in the center of the main cylinder. Three different diameters—10 mm, 25 mm, and 50 mm—are chosen as typical examples, and the ratios of the main cylinder are 0.1, 0.25, and 0.5, respectively. The other structural and operational parameters are all the same. The inlet velocity is 2 m/s, and the overflow split ratio is 0.2.

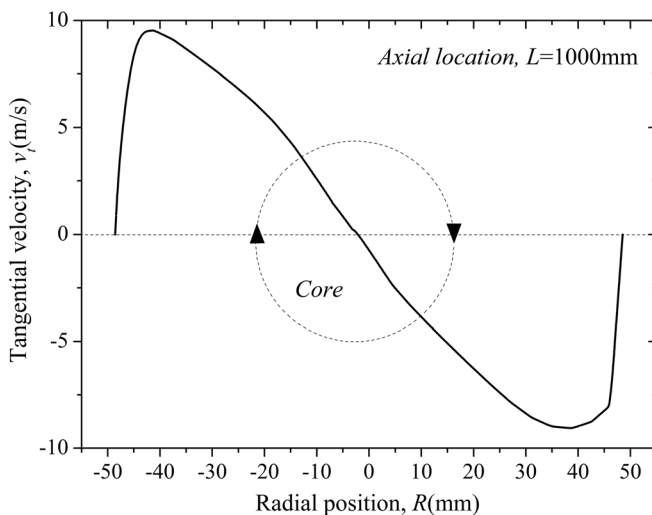


FIG. 5. The distribution of tangential velocity in the cross section of the main cylinder.

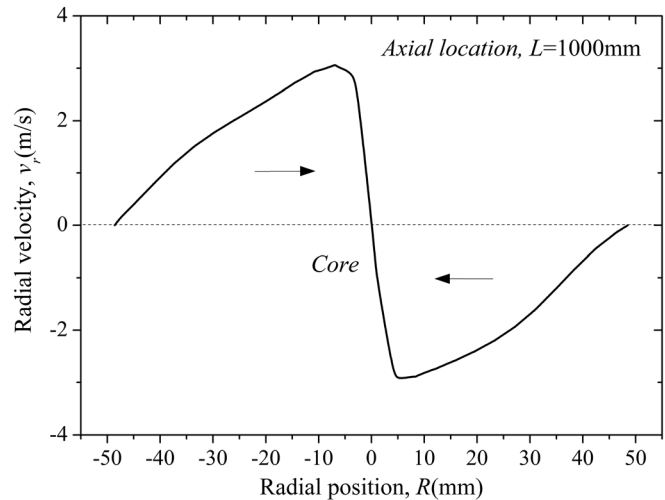


FIG. 6. The distribution of radial velocity in the cross section of the main cylinder.

The vortex structure in the cores of cylinders with overflow pipes of different diameters is shown in Fig. 8. The axial velocity in the main cylinder is limited to 0–10 m/s to distinguish the shape of the vortex core. We can see that the structure of the vortex core in the main cylinder of the cylindrical cyclone is not a regular cylinder. The shape of the vortex core is influenced by the swirling flow field. However, the overall structure of the vortex core is an axisymmetric shape, and the diameter is approximate equal along the length of the vortex except the tail. Therefore, the vortex core is reduced to a cylinder in the analysis of the separation process. The results show that the diameter of the overflow pipe has a great influence on the equivalent length of the vortex core, which is 998 mm, 534 mm, and 495 mm when the diameter of the overflow pipe is 10 mm, 25 mm, and 50 mm, respectively. The length of the vortex core is always the same as the main cylinder when the diameter of the overflow pipe is 10 mm. Therefore, an overflow pipe with a small diameter is advantageous for oil-water two-phase

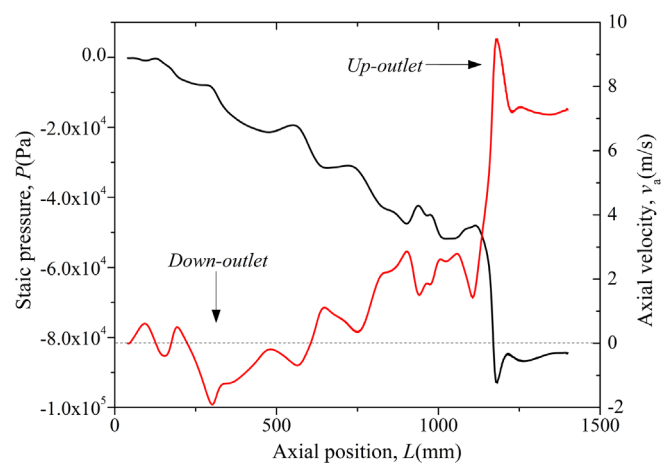
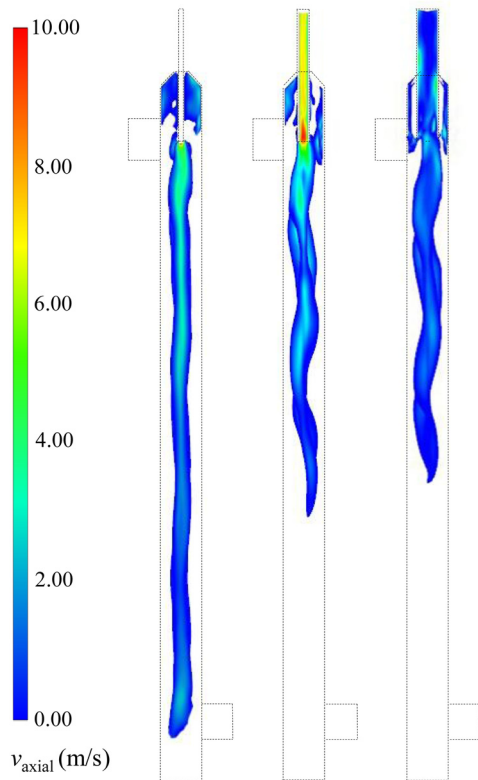


FIG. 7. The distribution of static pressure and axial velocity in the axial line of the main cylinder.



**FIG. 8.** The vortex structure in the cores of cylinders with overflow pipes of different diameters ( $D_{\text{over}} = 10$  mm, 25 mm, and 50 mm).

separation in a cylindrical cyclone if the pressure drop and overflow velocity are not considered. According to the dimension analysis, the relation between the length of the vortex core and the diameter of the overflow pipe can be described as follows:

$$\frac{L_{\text{core}}}{D_m} \propto \left( \frac{D_{\text{over}}}{D_m} \right)^m, \quad (17)$$

where the value of  $m$  is less than zero, which can be obtained from the series of numerical simulations or experiments.

Figure 9 gives the distribution of the axial velocity in the cross sections of main cylinders with different sizes of overflow pipe. The axial location of the cross section from the bottom in the main cylinder is 1000 mm. We can see that the distributions of axial velocity are almost identical for the three sizes of overflow pipe. The critical boundary of the axial velocity between the upward and downward two directions is similar. The axial velocity is upward in the core and downward near the wall of the main cylinder. The equivalent diameter of the vortex core in the center is about 46 mm, and the ratio of the vortex core to the main cylinder is 0.46. Thus, the influence of the diameter of the overflow pipe on the diameter of the vortex core can be ignored.

### C. The influence of the inlet velocity

In this section, we consider the effect of the inlet velocity on the structure of the vortex core in the center of the main cylinder. A series

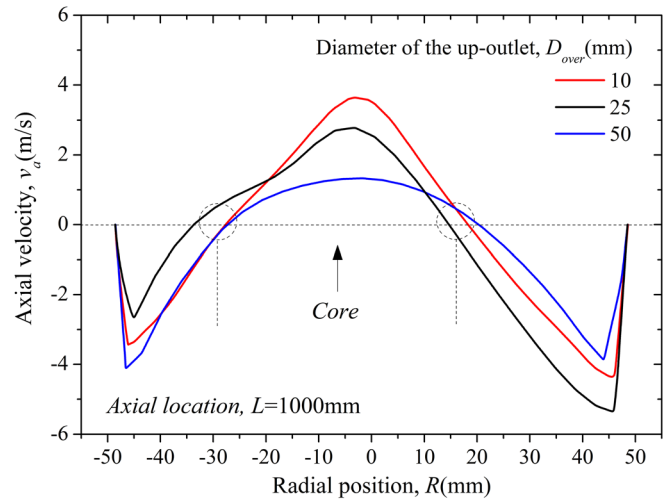


**FIG. 9.** The distribution of axial velocity in the cross sections of cylinders with different sizes of vortex finder.

of inlet velocities from 1 m/s to 5 m/s are entered into the numerical simulation. The structural parameters of the cylindrical cyclone with vortex finder are shown in Table I. The diameter of the up-outlet is 25 mm, and the overflow split ratio is set to 0.2.

The vortex structure in the cores of cylinders with different inlet velocities is given in Fig. 10. The axial velocity in the main cylinder is limited to 0–10 m/s to clearly distinguish the shape of the vortex core. The results show that the inlet velocity has little influence on the equivalent length of the vortex core, which is 547 mm, 534 mm, and 542 mm for inlet velocities of 1 m/s, 2 m/s, and 5 m/s. Therefore, the influence of the inlet velocity on the length of the vortex core can be ignored (Fig. 11).

### D. The influence of the overflow split ratio

In this section, we consider the influence of the flow split ratio of the two outlets on the structure of the vortex core in the center of the main cylinder. A series of overflow split ratios are set on the boundary conditions of the numerical simulation. The structural parameters of the cylindrical cyclone with vortex finder are shown in Table I. The diameter of the up-outlet is 25 mm, and the inlet velocity is set to 2 m/s.

Figure 12 shows the effects of different overflow split ratios on the shape of the vortex core in the center of the main cylinder. The axial velocity in the main cylinder is limited to 0–10 m/s to clearly distinguish the shape of the vortex core. The results show that the overflow split ratio has a distinct influence on the length of the vortex core: The length increases as the overflow split ratio increases. The influence of the overflow split ratio on the length of the vortex core is shown in Fig. 13. When the overflow split ratio is in the range 0.1–0.5, the unit of the length of the vortex core is millimeters:

$$L_{\text{core}} = 1038 \times \lambda_{\text{over}}^{0.39} \quad (0.1 \leq \lambda_{\text{over}} \leq 0.5). \quad (18)$$

Following the results of the mechanism analysis in Sec. II, this relationship can be rewritten as a dimensionless one. It is important to analyze

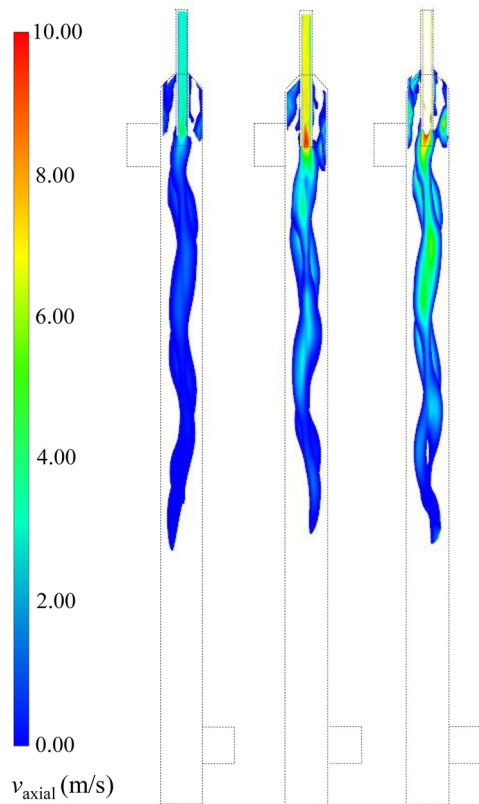


**FIG. 10.** The vortex structure in the cores of cylinders with different inlet velocities ( $V_{inlet} = 1.0$  m/s, 2.0 m/s, and 5.0 m/s).

the process of oil-water two-phase separation in cylindrical cyclones with vortex finders:

$$\frac{L_{core}}{D_m} \propto \lambda_{over}^{0.39} (0.1 \leq \lambda_{over} \leq 0.5). \quad (19)$$

The influence of the overflow split ratio on the distribution of the axial velocity in the cross section of the main cylinder is shown in Fig. 14. The axial location of the cross section from the bottom in the main cylinder is 1000 mm. The distributions of axial velocity are almost identical. Also, the equivalent diameter of the vortex core in the center is about 46 mm. Thus, the effect of the flow split ratio on the diameter of the vortex core can be ignored.

## V. ANALYSIS OF OIL-WATER SEPARATION

As the results above show, the structure of a cylindrical cyclone with vortex finder can be used to realize two-phase separation. To determine the characteristics of separation in a cylindrical cyclone with vortex finder, we consider here oil-water two-phase separation. The effects of structural parameters of the cylindrical cyclone on two-phase separation can be obtained from the flow field distribution; the flow and control parameters considered here include the diameter of the oil droplet, the flow split ratio, and the inlet velocity. The diameter of the overflow pipe is 25 mm. Moreover, the separation efficiency  $\eta$  is introduced to quantify the oil-water two-phase separation:<sup>30</sup>

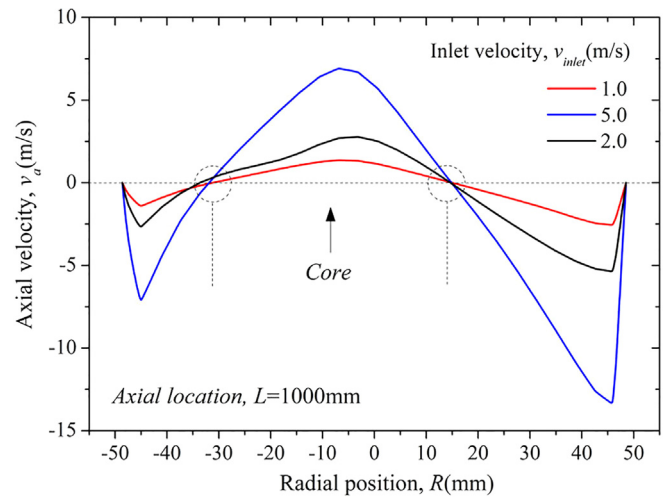


**FIG. 11.** The distribution of axial velocity in the cross sections of cylinders with different inlet velocities.

$$\eta = \left| \frac{Q_{o,up-outlet}}{Q_{o,inlet}} - \frac{Q_{w,up-outlet}}{Q_{w,inlet}} \right| \times 100\%. \quad (20)$$

Here,  $Q_{o,up-outlet}$  and  $Q_{o,inlet}$  are the oil flow rate in the up-outlet and inlet of the cylindrical cyclone in  $m^3/h$ , and  $Q_{w,up-outlet}$  and  $Q_{w,inlet}$

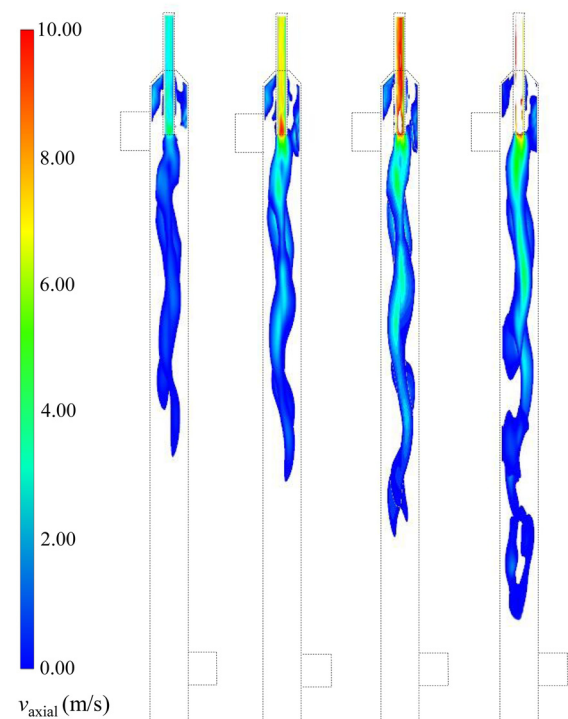


**FIG. 12.** The vortex structure in the cores of cylinders with different overflow split ratios ( $\lambda_{over} = 0.1, 0.2, 0.3, \text{ and } 0.5$ ).



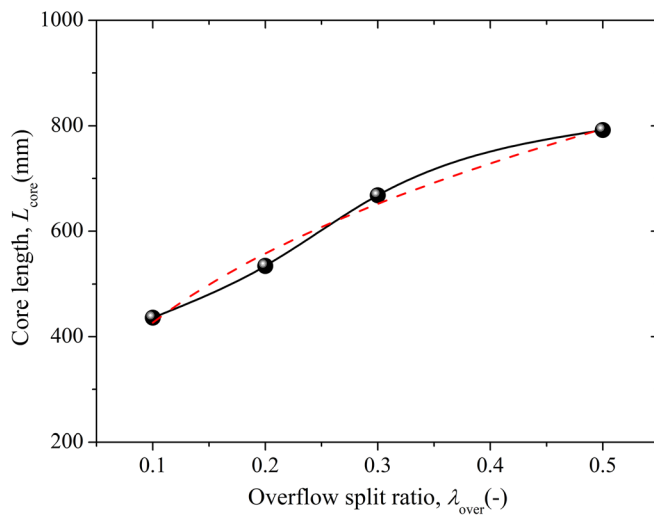


**FIG. 13.** The effect of the overflow split ratio on the length of the core in a cylindrical cyclone.

are the water flow rate in the up-outlet and inlet of the cylindrical cyclone in  $\text{m}^3/\text{h}$ .

The effects of the inlet oil droplet diameter on oil-water two-phase separation are given in Figs. 15 and 16. The overflow split ratio is 0.1, and the inlet mixture velocity and oil volume fraction are 3 m/s and 0.1, respectively. Figure 15 shows the distribution of the oil phase in cylindrical cyclones with different inlet oil droplet diameters. It shows that the diameter of the oil droplet has a great influence on the phase distribution, especially on the core of the cylinder. The oil volume fraction in the core increases as the inlet oil droplet diameter increases from 0.05 mm to 1 mm. It is important to oil-water two-phase separation. The effects of the inlet oil droplet diameter on the separation efficiency and the oil volume fractions in the up- and

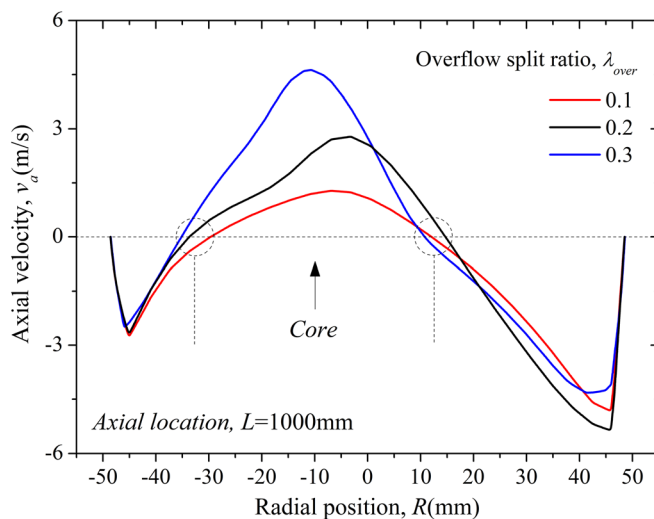


**FIG. 14.** The distribution of axial velocity in cross sections with different overflow split ratios.

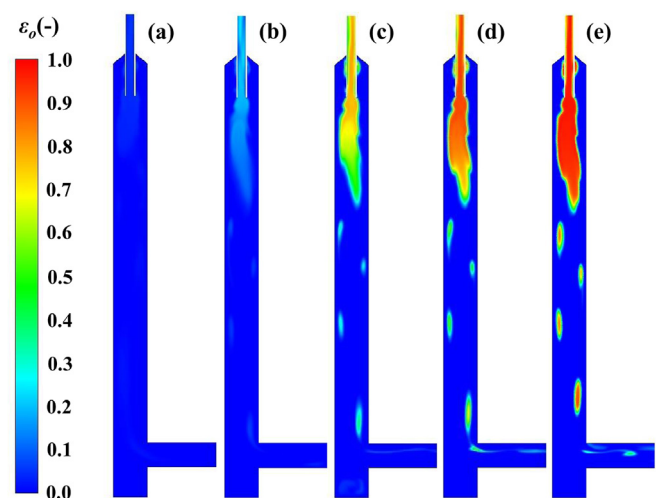


**FIG. 15.** The distribution of the oil phase in cylindrical cyclones with different inlet oil droplet diameters ( $d_{o,in} = 0.05$  mm, 0.1 mm, 0.3 mm, 0.5 mm, and 1 mm).

down-outlets are shown in Fig. 16. We can see that the oil volume fraction increases in the up-outlet but decreases in the down-outlet as the inlet oil droplet diameter increases. In other words, the oil-water separation increases as the diameter of the oil droplet increases. The change in the separation efficiency with oil droplets of different diameters can be used to measure this clearly. The separation efficiency of a cylindrical cyclone with vortex can reach 80% if the inlet dispersion droplet diameter is larger than 1 mm.

The flow split ratio has a great influence on the flow field in a cylindrical cyclone, which in turn influences separation. The effects of the up-outlet flow split ratio on separation are given in Figs. 17 and 18. The inlet oil droplet diameter is set to 0.1 mm, and the inlet mixture velocity and oil volume fraction are 3 m/s and 0.1, respectively. The distribution of the oil phase in cylindrical cyclones with different up-outlet flow split ratios of 0.05, 0.1, 0.2, and 0.3 is shown in Fig. 17. We

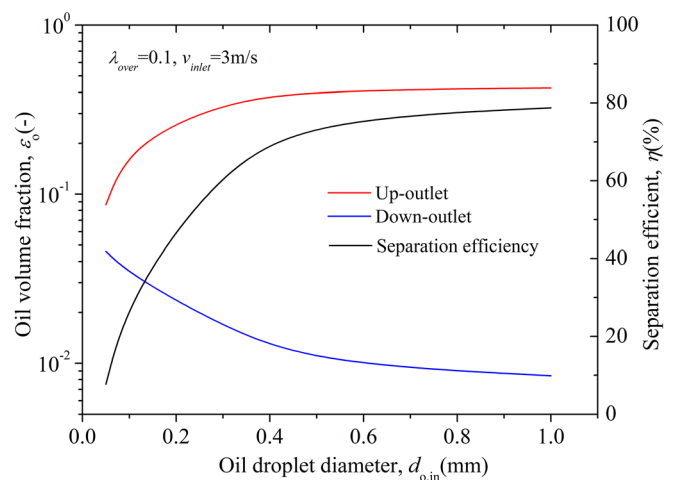


**FIG. 16.** Effects of the inlet oil droplet diameter on separation in a cylindrical cyclone.

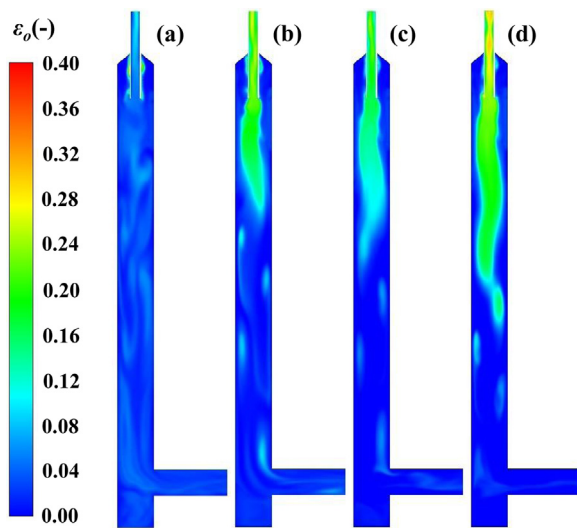


FIG. 17. The distribution of the oil phase in cylindrical cyclones with different flow split ratios ( $\lambda_{over} = 0.05, 0.1, 0.2$ , and  $0.3$ ).

can see that the distribution is always the same as the structure of the vortex core in the cylinder compared to Fig. 12. The effects of the up-outlet flow split ratio on the separation efficiency and oil volume fractions in the up- and down-outlets are shown in Fig. 18. The oil volume fractions in the up- and down-outlets decrease as the up-outlet flow split ratio increases. However, the separation efficiency increases when the up-outlet flow split ratio is smaller than  $0.3$ . In practice, the separation efficiency and the oil volume fractions in the up- and down-outlets are used to measure the results of different separation requests. The flow split ratio is the only operating parameter to consider to obtain the best separation results for a cylindrical cyclone with a fixed inlet oil-water mixture.

An optimum application range exists for the cylindrical cyclone. Thus, we study a series of inlet mixture velocities. The phase distribution in cylindrical cyclones with different inlet velocities is shown in Fig. 19.

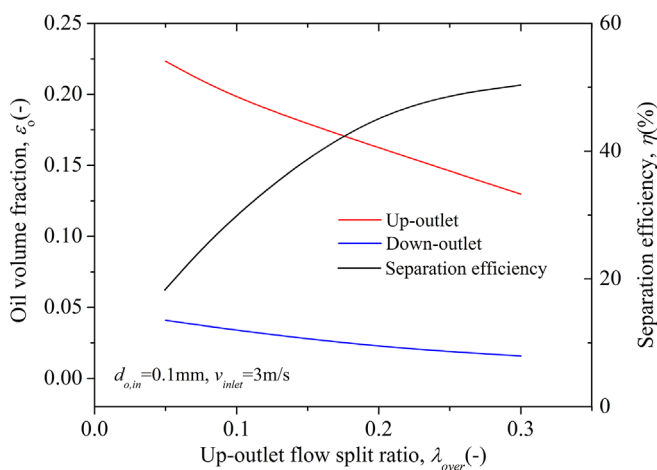


FIG. 18. Effects of the flow split ratio on separation in a cylindrical cyclone.

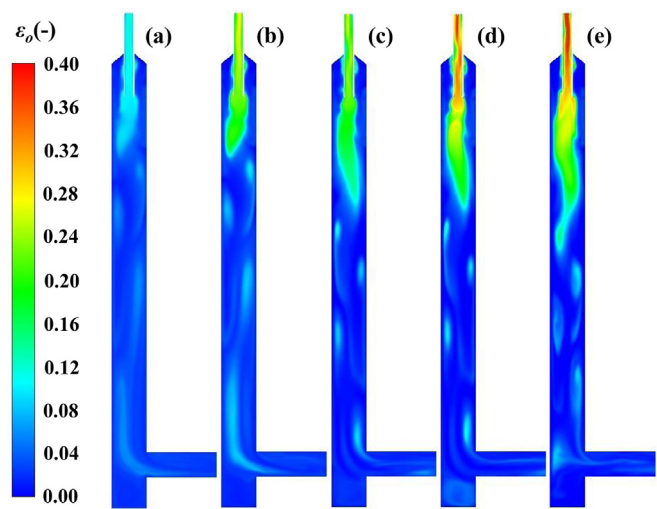


FIG. 19. The distribution of the oil phase in cylindrical cyclones with different inlet mixture velocities ( $v_{inlet} = 1 \text{ m/s}, 2 \text{ m/s}, 3 \text{ m/s}, 5 \text{ m/s}$ , and  $7 \text{ m/s}$ ).

The other flow and operating parameters are the same to each other. The up-outlet flow split ratio is  $0.1$ , and the inlet oil droplet diameter and volume fraction are set to  $0.1 \text{ mm}$  and  $0.1$ , respectively. We can see that the oil volume fraction in the vortex core varies with the centrifugal acceleration generated with different inlet velocities. The effects of the inlet velocity on the separation efficiency and the oil volume fractions in the up- and down-outlets are shown in Fig. 20. The oil volume fraction increases in the up-outlet but decreases in the down-outlet as the inlet velocity increases. Moreover, the separation efficiency first increases and then decreases as the inlet velocity increases from  $1 \text{ m/s}$  to  $7 \text{ m/s}$ . The maximum separation efficiency is about  $40\%$  when the inlet velocity is  $5.6 \text{ m/s}$ . Presently, the designed cylindrical cyclone with vortex finder has been tested in the petroleum industry. It can realize the oil-water separation greatly, and the separated efficiency and energy consumption are better than the traditional gravity separator.

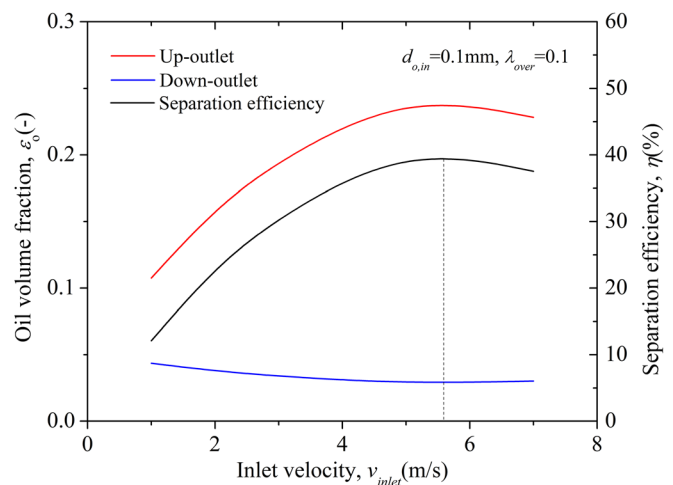


FIG. 20. Effects of the inlet mixture velocity on separation in a cylindrical cyclone.

## VI. CONCLUSION

Here, we use dimensional analysis and multiphase flow numerical simulation to analyze separation in a cylindrical cyclone with the vortex finder. The flow field and transport of dispersed droplets in the cylindrical cyclone are researched systematically. The axial, tangential, and radial velocities in the cylinder are described. It is important to understand the process and principle behind separation. There is a vortex in the core of the cylinder, and its structure is influenced by the diameter of the overflow pipe, the inlet velocity, and the flow split ratio. The influence of the diameter of the overflow pipe, the inlet velocity, and the flow split ratio on the diameter of the vortex core can be ignored. The equivalent length of the vortex core in the cylindrical cyclone can be obtained from the relation below:

$$\frac{L_{core}}{D_m} \propto \left( \frac{D_{over}}{D_m} \right)^m, \lambda_{over}^n. \quad (21)$$

In this work,  $m$  and  $n$  are 0.46 and 0.39, respectively. It is useful to analyze the process and efficiency of oil-water two-phase separation. To obtain the characteristics of separation in the cylindrical cyclone with vortex finder, we study oil-water two-phase separation. The effects of the inlet oil droplet diameter, flow split ratio, and inlet velocity are studied with multiphase flow numerical simulation. In practice, the separation efficiency and the oil volume fractions in the up- and down-outlets are used to measure the results of different separation requests. Oil-water separation increases as the diameter of the oil droplet increases. The separation efficiency of a cylindrical cyclone with vortex can reach 80% if the inlet dispersion droplet diameter is larger than 1 mm. The oil volume fractions in the up- and down-outlets decrease as the up-outlet flow split ratio increases. The flow split ratio is the only operating parameter to consider to obtain the best separation results for a cylindrical cyclone with a fixed inlet oil-water mixture. The oil volume fraction increases in the up-outlet but decreases in the down-outlet as the inlet velocity increases. The maximum separation efficiency is about 40% when the inlet velocity is 5.6 m/s. It is important to design cylindrical cyclones with vortex finders optimally for applications in the petroleum industry.

## ACKNOWLEDGMENTS

This work was supported by the National Natural Science Foundation of China (Grant Nos. 11972039 and 51509235).

## AUTHOR DECLARATIONS

### Conflict of Interest

The authors have no conflicts to disclose.

## DATA AVAILABILITY

The data that support the findings of this study are available from the corresponding author upon reasonable request.

## REFERENCES

- <sup>1</sup>R. I. Dekker, A. Deblais, B. Veltkamp, P. Veenstra, W. K. Kegel, and D. Bonn, "Creep and drainage in the fast destabilization of emulsions," *Phys. Fluids* **33**, 033302 (2021).
- <sup>2</sup>H. S. Skjefstad, M. Dudek, G. Oye, and M. Stanko, "The effect of upstream inlet choking and surfactant addition on the performance of a novel parallel pipe oil-water separator," *J. Petrol. Sci. Eng.* **189**, 106971 (2020).
- <sup>3</sup>Y. Tian, Y. Tian, G. Shi, B. Zhou, C. Zhang, and L. He, "Experimental study on oil droplet breakup under the action of turbulent field in modified concentric cylinder rotating device," *Phys. Fluids* **32**, 087105 (2020).
- <sup>4</sup>N. K. G. Silva, D. O. Silva, L. G. M. Vieira, and M. A. S. Barrozo, "Effect of underflow diameter and vortex finder length on the performance of a newly designed filtering hydrocyclone," *Power Technol.* **286**, 305–310 (2015).
- <sup>5</sup>C. A. O. Araujo, C. M. Scheid, J. B. R. Loureiro, T. S. Klein, and R. A. Medronho, "Hydrocyclone for oil-water separations with high oil content: Comparison between CFD simulations and experimental data," *J. Petrol. Sci. Eng.* **187**, 106788 (2020).
- <sup>6</sup>J. Kou, Y. Chen, and J. Q. Wu, "Numerical study and optimization of liquid-liquid flow in cyclone pipe," *Chem. Eng. Proc.* **147**, 107725 (2020).
- <sup>7</sup>J. Y. Tian, L. Ni, T. Song, and J. N. Zhao, "CFD simulation of hydrocyclone-separation performance influenced by reflux device and different vortex-finder lengths," *Sep. Purif. Tech.* **233**, 116013 (2020).
- <sup>8</sup>E. Afanador, "Oil-water separation in liquid-liquid cylindrical cyclone separator," M.S. thesis, The University of Tulsa, 1999.
- <sup>9</sup>C. Oropeza-Vazquez, E. Afanador, L. Gomez, S. Wang, R. Mohan, O. Shoham, and G. Kouba, "Oil-water separation in a novel liquid-liquid cylindrical cyclone (LLCC) compact separator: Experiments and modeling," *J. Fluid Eng.* **126**, 553–564 (2004).
- <sup>10</sup>R. S. Mathiravedu, S. Wang, R. S. Mohan, O. Shoham, and J. D. Marrelli, "Performance and control of liquid-liquid cylindrical cyclone separators," *J. Energy Res. Technol.* **132**, 011001 (2010).
- <sup>11</sup>H. F. Liu, J. Y. Xu, Y. X. Wu, and Z. C. Zheng, "Numerical study on oil and water two-phase flow in a cylindrical cyclone," *J. Hydrodyn.* **22**(5), 832–837 (2010).
- <sup>12</sup>Z. Gao, J. Wang, Y. Mao, and Y. Wei, "Analysis of the effect of vortex on the flow field of a cylindrical cyclone separator," *Sep. Purif. Technol.* **211**, 438–447 (2019).
- <sup>13</sup>I. Mokni, H. Dhaouadi, P. Bournot, and H. Mhiri, "Numerical investigation of the effect of the cylindrical height on separation performances of uniflow hydrocyclone," *Chem. Eng. Sci.* **122**, 500–513 (2015).
- <sup>14</sup>M. P. Boruah, A. Sarker, P. R. Randive, S. Pati, and K. C. Sahu, "Tuning of regimes during two-phase flow through a cross-junction," *Phys. Fluids* **33**, 122101 (2021).
- <sup>15</sup>J. Lai, L. Sun, L. Gao, T. Tan, and P. Li, "Two-phase flow-induced instability and nonlinear dynamics of a rotated triangular tube array in parallel direction," *Eur. J. Mech. Solid.* **83**, 104024 (2020).
- <sup>16</sup>Z. W. Gao, J. Wang, J. Y. Wang, and Y. Mao, "Time-frequency analysis of the vortex motion in a cylindrical cyclone separator," *Chem. Eng. J.* **373**, 1120–1131 (2019).
- <sup>17</sup>F. Drui, A. Larat, S. Kokh, and M. Massot, "Small-scale kinematics of two-phase flows: Identifying relaxation processes in separated- and dispersed-phase flow models," *J. Fluid Mech.* **876**, 326–355 (2019).
- <sup>18</sup>T. A. Barber and J. Majdalani, "On the Beltraman motion of the bidirectional vortex in a conical cyclone," *J. Fluid Mech.* **828**, 708–732 (2017).
- <sup>19</sup>S. Y. Shi, Y. X. Wu, J. Zhang, J. Guo, and S. J. Wang, "A study on separation performance of a vortex finder in a liquid-liquid cylindrical cyclone," *J. Hydrodyn.* **22**(5), 391–397 (2010).
- <sup>20</sup>M. Ghodrat, S. B. Kuang, A. B. Yu, A. Vince, G. D. Barnett, and P. J. Barnett, "Numerical analysis of hydrocyclones with different vortex finder configurations," *Miner. Eng.* **63**, 125–138 (2014).
- <sup>21</sup>I. Mantilla, S. Shirazi, and O. Shoham, "Flow field prediction and bubble trajectory model in GLCC separators," *ASME J. Energy Resour. Technol.* **121**, 9–14 (1999).
- <sup>22</sup>A. Clausse and M. L. Bertodano, "Natural modes of the two-fluid model of two-phase flow," *Phys. Fluids* **33**, 033324 (2021).
- <sup>23</sup>Y. Zhang, X. B. Lu, and X. H. Zhang, "An optimized Eulerian–Lagrangian method for two-phase flow with coarse particles: Implementation in open-

- source field operation and manipulation, verification, and validation,” *Phys. Fluids* **33**, 113307 (2021).
- <sup>24</sup>S. Liu, J. Zhang, L. T. Hou, and J. Y. Xu, “Investigation on the variation regularity of the characteristic droplet diameters in the swirling flow field,” *Chem. Eng. Sci.* **229**, 116153 (2021).
- <sup>25</sup>J. Lai, D. Zhang, L. Sun, L. Guo, T. Tan, and P. Li, “Investigation on fluidelastic instability of tube bundles considering the effect of slip ratio of air-water two-phase flow,” *Ann. Nucl. Energy* **144**(5), 107530 (2020).
- <sup>26</sup>J. Lai, S. Yang, T. Tan, and L. Sun, “The influence of internal flow on the non-linear dynamics of a flexible tube in tube bundles subjected to two-phase cross-flow,” *Ann. Nucl. Energy* **165**(2), 108684 (2022).
- <sup>27</sup>S. Heinz, R. Mokhtarpour, and M. Stoellinger, “Theory-based Reynolds-averaged Navier–Stokes equations with large eddy simulation capability for separated turbulent flow simulation,” *Phys. Fluids* **32**, 065102 (2020).
- <sup>28</sup>A. Escue and J. Cui, “Comparison of turbulence models in simulating swirling pipe flows,” *Appl. Math. Mod.* **34**, 2840–2849 (2010).
- <sup>29</sup>X. S. Zhang, J. H. Wang, and D. C. Wan, “Euler–Lagrange study of bubble drag reduction in turbulent channel flow and boundary layer flow,” *Phys. Fluids* **32**, 027101 (2020).
- <sup>30</sup>L. L. Yang, J. Zhang, Y. Ma, J. Y. Xu, and J. Wang, “Experimental and numerical study of separation characteristics in gas-liquid cylindrical cyclone,” *Chem. Eng. Sci.* **214**, 115362 (2020).